EMBO reports

TRANSPARENT PROCESS

scientific report

# Cuf2 boosts the transcription of APC/C activator Fzr1 to terminate the meiotic division cycle

*Yuki Aoi*[1,2], *Kunio Arai*[2], *Masaya Miyamoto*[2], *Yuji Katsuta*[2†], *Akira Yamashita*[1], *Masamitsu Sato*[2,3+‡] *& Masayuki Yamamoto*[1,2++]

[1]Laboratory of Gene Function, Kazusa DNA Research Institute, Chiba, [2]Department of Biophysics and Biochemistry, Graduate School of Science, University of Tokyo, Tokyo, and [3]PRESTO, Japan Science and Technology Agency, Saitama, Japan

**The number of nuclear divisions in meiosis is strictly limited to two. Although the precise mechanism remains unknown, this seems to be achieved by adjusting the anaphase-promoting complex/cyclosome (APC/C) activity to degrade cyclin. Here, we describe a fission yeast *cuf2* mutant that enters into a third nuclear division cycle, represented by ectopic spindle assembly and abnormal chromosome segregation. Cuf2 is a meiotic transcription factor, and its critical target is *fzr1*$^+$*/mfr1*$^+$, which encodes a meiotic APC/C activator. *fzr1*Δ also enters a third nuclear division. Thus, Cuf2 ensures termination of the M-phase cycle by boosting Fzr1 expression to generate functional gametes.**

Keywords: APC/C; Cdk; cell cycle; cyclin destruction; meiosis

EMBO *reports* (2013) **14,** 553–560. doi:10.1038/embor.2013.52

## INTRODUCTION

Diploid germ line cells must undergo exactly two divisions to produce functional haploid gametes through meiosis. To achieve this specialized cell cycle programme, the activity of cyclin-dependent kinase Cdk1 appears to be tightly controlled during meiosis [1–4]. In the fission yeast *Schizosaccharomyces pombe*, it has been shown that the Mes1 protein inhibits full activation of the anaphase-promoting complex/cyclosome (APC/C) after meiosis I by blocking binding of substrates to the APC/C activators Slp1/Cdc20/Fizzy and Fzr1/Mfr1/Fizzy-related, to protect a portion of Cdc13/cyclin B from proteolysis by APC/C [5,6]. In contrast, termination of meiotic divisions is thought to be dependent on activation of APC/C by the meiosis-specific APC/C activator Fzr1/Mfr1/Fizzy-related [7], which corresponds to Ama1 in budding yeast [8]. However, the main phenotype of the mutants defective in these APC/C activators is deficiency in spore wall formation rather than in cell cycle termination. Therefore, it remains unclear how the division cycle is terminated accurately after the second meiotic division. We investigated this issue using the *mes1* mutant, which shows premature termination of meiosis.

[1]Laboratory of Gene Function, Kazusa DNA Research Institute, 2-6-7 Kazusa-kamatari, Kisarazu, Chiba 292-0818, Japan
[2]Department of Biophysics and Biochemistry, Graduate School of Science, University of Tokyo, 7-3-1 Hongo, Bunkyo-ku, Tokyo 113-0033, Japan
[3]PRESTO, Japan Science and Technology Agency, 4-1-8 Honcho, Kawaguchi, Saitama 332-0012, Japan
[†]Present address: Shiseido Research Centre, 2-2-1 Hayabuchi, Tsuzuki-ku, Yokohama, Kanagawa 224-8558, Japan
[‡]Present address: Department of Life Science and Medical Bioscience, School of Advanced Science and Engineering, Waseda University-TWIns, 2-2 Wakamatsucho, Shinjuku-ku, Tokyo 162-8480, Japan
[+]Corresponding author. Tel: +81 3 5369 7322; Fax: +81 3 5369 7322; E-mail: masasato@waseda.jp
[++]Corresponding author. Tel: +81 438 52 3944; Fax: +81 438 52 3911; E-mail: myamamoto@kazusa.or.jp

**Received 19 November 2012; revised 1 April 2013; accepted 2 April 2013; published online 30 April 2013**

## RESULTS AND DISCUSSION

### Isolation of *sms* mutants that suppress the *mes1* mutation

We performed a genetic screen to search for factors that might regulate the termination of meiosis. Our strategy is illustrated in Fig 1A. Wild-type (WT) diploid cells produce four-spore asci (sac-like structures that contain spores in fungi) after two rounds of meiotic division, but the *mes1* mutant terminates meiosis after the first division, producing binucleate cells without the spore wall. We introduced random mutations into the *mes1* mutant, and chose mutants in which the early termination phenotype was suppressed and the second division and sporulation were resumed. We termed such mutants *sms* (suppressor of *mes1*). Nine independent *sms* mutants (*sms1*–*sms9*) were isolated; the typical phenotype of *mes1 sms5* cells is shown in Fig 1B. Hereafter, we focus on *sms1* and *sms5*. Nearly half of *mes1 sms1* and *mes1 sms5* mutant cells produced four spores in an ascus, whereas the *mes1* single mutant never formed spores (Figs 1B,C). Thus, functional Sms1 and Sms5 were expected to act as factors to terminate meiosis.

### The *cuf2* and *fzr1* mutants fail to terminate meiosis

Whole-genome sequencing and subsequent analyses indicated that the *sms1* gene responsible for the suppressor phenotype was identical to *fzr1*$^+$*/mfr1*$^+$. The *sms1* mutant contained a mutation in the promoter region of the *fzr1/mfr1* gene. Previous studies suggested that Fzr1/Mfr1 is required to decrease Cdc13 levels after meiosis II [7]. Deletion of *fzr1* (*fzr1*Δ) was shown to suppress meiotic defects of the *mes1*Δ mutant [9,10]. Fzr1 has been implicated in spore morphogenesis: *fzr1*Δ was delayed in spore formation and produced aberrant asci [7,11]. Nascent *fzr1*Δ

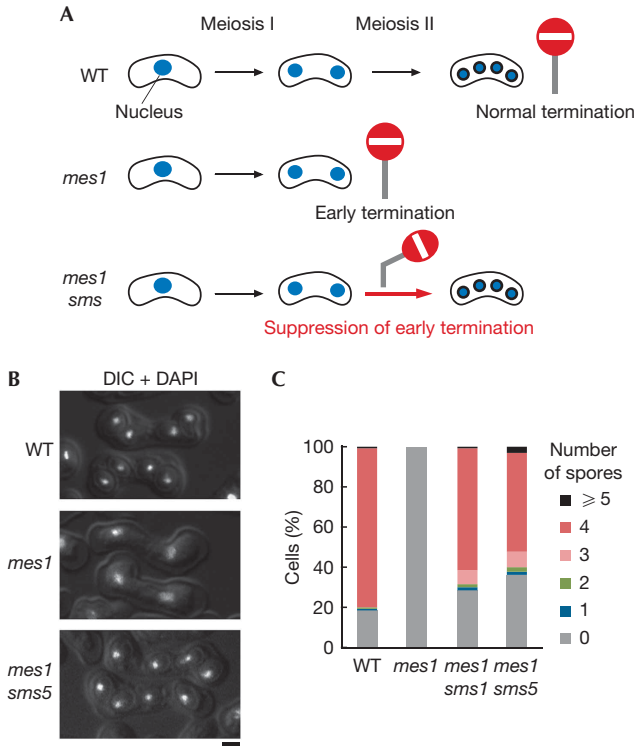


**Fig 1** | Screen for mutants that counteract early termination of meiosis. (**A**) Scheme illustrating the screening strategy. The *mes1* mutant arrests before meiosis II 'early termination' and generates no spores. Mutations were introduced randomly into the *mes1* mutant, and mutants in which the 'early termination' phenotype was suppressed and meiosis II and sporulation occurred were chosen. (**B**) Suppression of *mes1* by the *sms5* mutation. Mating and meiosis were induced in WT, *mes1* and *mes1 sms5* cells. They were stained with DAPI and merged images of fluorescence microscopy and DIC are shown. Scale bar, 2 μm. (**C**) Distribution of the number of spores produced by each zygote was measured for the WT, *mes1*, *mes1 sms1*, and *mes1 sms5* strains incubated on SPA at 25 °C for 24 h ($n > 200$ for each strain). Percentages were calculated on a diploid zygotic cell basis. DAPI, 4',6-diamidino-2-phenylindole; DIC, differential interference contrast; *sms*, suppressor of *mes1;* SPA, sporulation agar; WT, wild type.

prespores were irregularly shaped and the outer layer of spore walls was often missing, although structural alteration of the spindle pole body (SPB) required for spore formation occurred normally [11]. *fzr1*Δ cells completed meiosis II normally but they remained with high levels of Cdc13 and Cdk activity at the end of meiosis, and cells overexpressing a non-degradable Cdc13 mutant mimicked the sporulation-defective phenotype of *fzr1*Δ, leading to a proposal that rapid degradation of Cdc13 by APC/C–Fzr1 was required for the coordination of exit from meiosis and spore formation, by analogy with the coordination of mitotic exit and cytokinesis [7]. These previous studies, however, did not pay precise attention to the defects of *fzr1*Δ in terms of cell cycle progression (see below).

The *sms5* gene was shown to be allelic to *cuf2*$^+$, which encodes a meiotically upregulated transcription factor [12,13]. Cuf2 was also independently identified as a homologue of the copper-regulatory transcription factor Cuf1. The *cuf2*Δ mutant has been shown to have an alteration in meiotic transcriptome and defects in spore wall formation [13]. We noticed a new meiotic phenotype of the *cuf2*Δ mutant, that is, 19% of the cells exhibited abnormal nuclear distribution with more than four nuclei per cell, whereas most WT cells contained four nuclei (Fig 2A). Similar abnormal nuclei were observed in 39% of the *fzr1*Δ cells (Fig 2A), as reported previously [7,11]. This phenotype was barely strengthened in the *cuf2*Δ *fzr1*Δ double mutant (40%, Fig 2A). These results suggested that Cuf2 might play a new function to achieve proper divisions during meiosis in the same pathways as Fzr1/Mfr1.

To clarify how the abnormality of *cuf2* was generated, we performed tricolour live-cell imaging during meiosis, visualising microtubules in green by GFP–Atb2 (α2-tubulin), chromatin in blue by Htb1–CFP (histone H2B) and SPBs in red by Sfi1–mCherry (a half-bridge protein). The WT strain with these markers underwent meiosis II normally, in which the spindle segregated chromosomes in anaphase II and was then disassembled (Fig 2B; supplementary Movie S1 online). The *cuf2*Δ mutant also underwent normal meiotic divisions until four nuclei were produced (0 min, Fig 2C; supplementary Movie S2 online). After spindle disassembly in meiosis II, however, the SPBs started to assemble microtubules again (40 min) and chromosomes were partly segregated, giving rise to the fifth cluster of chromosomes

**Fig 2** | *cuf2*Δ and *fzr1*Δ cells show a defect in meiotic termination. (**A**) WT, *cuf2*Δ, *fzr1*Δ and *cuf2*Δ *fzr1*Δ cells were inoculated onto SPA and the number of nuclei generated in each zygote was counted after incubation at 30 °C for 24 h. Percentages were calculated on a diploid zygotic cell basis. The frequencies of cells with ⩾5 nuclei in *fzr1*Δ and *cuf2*Δ*fzr1*Δ were not significantly different ($P = 0.79$; Student's *t*-test). Data are averages of three independent experiments. (**B**,**C**) Abnormal reassembly of spindle microtubules and additional nuclear divisions were observed after meiosis II in the *cuf2*Δ and *fzr1*Δ strains. Time-lapse images of cells expressing GFP–Atb2 (microtubules; green), Htb1–CFP (histone H2B; blue) and Sfi1–mCherry (SPB; red) were filmed from meiosis II. (**B**) WT, (**C**) *cuf2*Δ. Movies corresponding to these panels are given in supplementary Movies S1 and S2 online. Images for *fzr1*Δ are shown in supplementary Fig S1A online. (**D**) Percentages of WT, *cuf2*Δ and *fzr1*Δ cells that formed ectopic spindles after meiosis II. Some cells also showed nuclear division. Cells were incubated on SPA at 25 °C for 24 h. (**E**,**F**) Additional duplication of SPBs and bipolar spindle formation in *fzr1*Δ cells. Time-lapse images of cells expressing GFP-Atb2, Mis6-2mRFP (kinetochore; red) and Sid4-2ECFP (SPB; blue) were filmed from meiosis II in WT (**E**) and *fzr1*Δ (**F**). Movies corresponding to these panels are given in supplementary Movies S3 and S4 online. Insets in (**F**), indicating a bipolar spindle with kinetochore alignment (a) and a monopolar spindle with SPB duplication (b), are magnified on the right. CFP, cyan fluorescent protein; ECFP, enhanced cyan fluorescent protein; GFP, green fluorescent protein; mRFP, monomeric red fluorescent protein; SPA, sporulation agar; SPB, spindle pole body; WT, wild type. Scale bar, 2 μm.

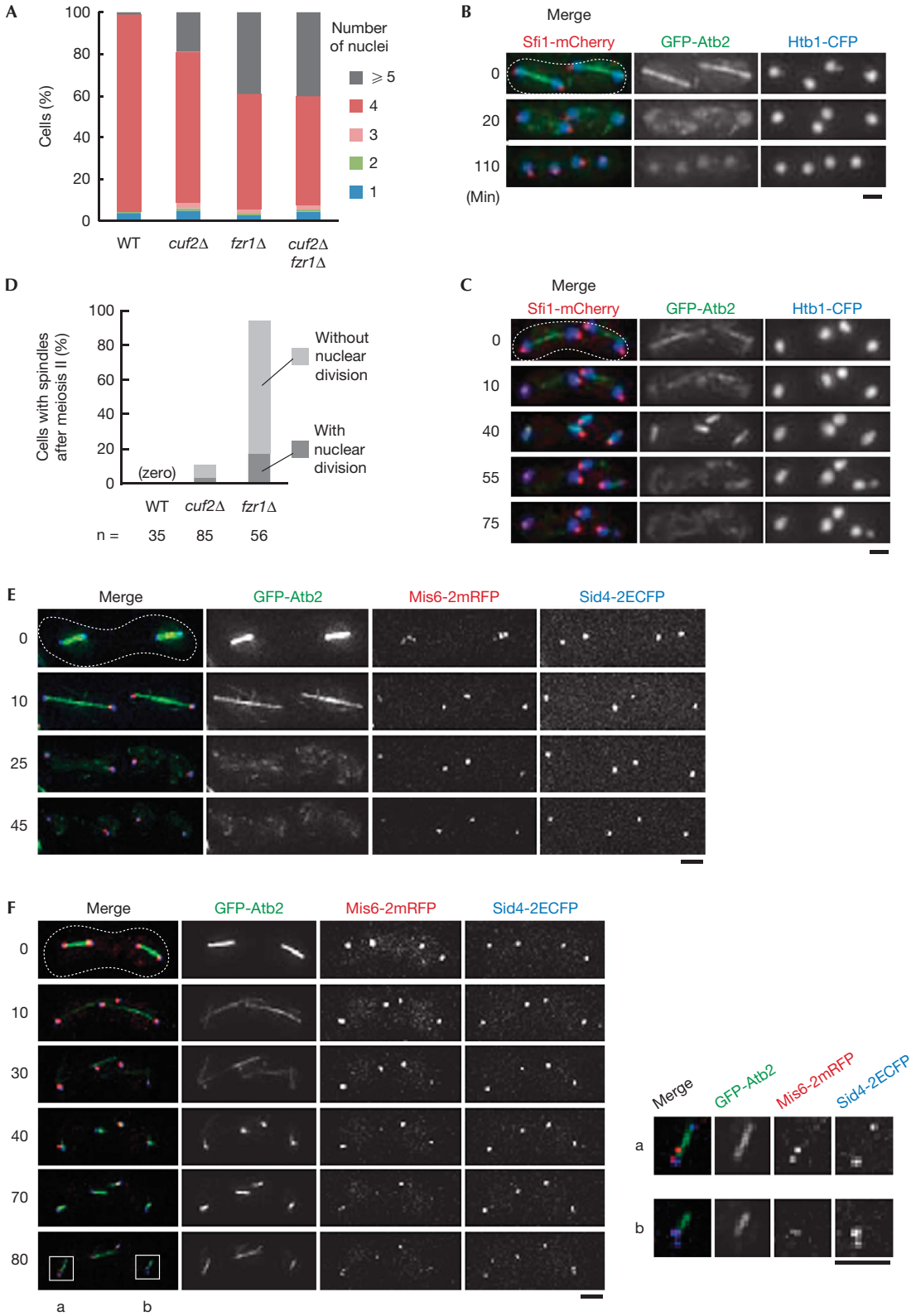
A
100
80
60
40
20
0
Cells (%)
Number of nuclei
⩾5
4
3
2
1
WT
cuf2Δ
fzr1Δ
cuf2Δ fzr1Δ
B
Merge
Sfi1-mCherry
GFP-Atb2
Htb1-CFP
0
20
110
(Min)
C
Merge
Sfi1-mCherry
GFP-Atb2
Htb1-CFP
0
10
40
55
75
D
Cells with spindles after meiosis II (%)
Without nuclear division
With nuclear division
(zero)
WT
cuf2Δ
fzr1Δ
n = 35 85 56
E
Merge
GFP-Atb2
Mis6-2mRFP
Sid4-2ECFP
0
10
25
45
F
Merge
GFP-Atb2
Mis6-2mRFP
Sid4-2ECFP
0
10
30
40
70
80
a
b
Merge
GFP-Atb2
Mis6-2mRFP
Sid4-2ECFP
a
b

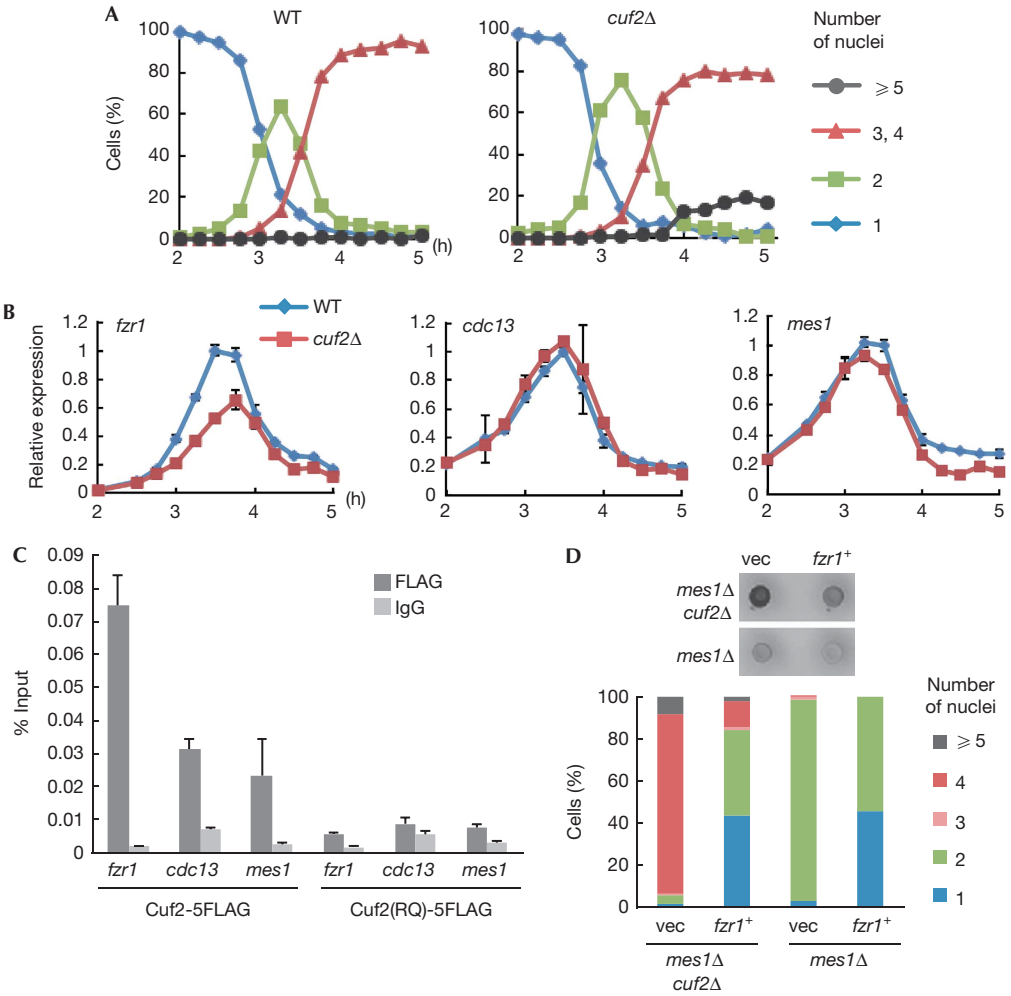


**Fig 3** | Cuf2 is a transcription factor required for *fzr1* expression. (**A**) Meiotic progression in synchronized WT and *cuf2*Δ cultures. Meiosis was induced using the *pat1-114* mutation, and the number of nuclei per cell was counted at each time point ($n > 200$). (**B**) Levels of *fzr1*, *cdc13* and *mes1* mRNAs at each time point were determined by quantitative RT–PCR in WT and *cuf2*Δ cells. Error bars represent s.d. (three reactions). The primary data were normalised by the *act1* mRNA levels. (**C**) ChIP assays. Cuf2–5FLAG or Cuf2(RQ)–5FLAG protein was immunoprecipitated from cells at meiosis I/meiosis II transition with the anti-FLAG antibody. Quantitative PCR was performed to measure the amounts of DNA fragments (promoter regions of respective genes) co-purified with each protein. Error bars represent s.d. (three reactions). (**D**) Suppression of the *mes1*Δ mutant by *cuf2*Δ was cancelled by overexpression of Fzr1. Either *mes1*Δ *cuf2*Δ or *mes1*Δ cells overexpressing *fzr1*$^+$ and control cells carrying only the vector were incubated on SPA to induce meiosis. (Top) Colonies that produced spore walls were detected with iodine vapour, which stained them brown. (Bottom) The number of nuclei generated in each zygote was counted ($n > 200$). Percentages were calculated on a diploid zygotic cell basis. ChIP, chromatin immunoprecipitation; SPA, sporulation agar; WT, wild type.

(55–75 min). This demonstrated that the *cuf2* mutant was defective in terminating nuclear divisions after meiosis II, and could enter 'the third division'-like phase.

We next investigated whether the meiosis III-like phenotype was also seen in the *fzr1*Δ mutant, which was previously reported to show abnormal nuclear divisions, although it was unknown how they were realized [7,11]. Interestingly, *fzr1*Δ mutant cells showed ectopic spindle formation for the meiosis III-like division at a higher frequency than *cuf2*Δ mutant cells (95% in *fzr1*Δ versus 11% in *cuf2*Δ cells) (Fig 2D). Similarly to the WT (25 min in WT, Fig 2E; supplementary Movie S3 online), the *fzr1*Δ cells performed normal nuclear divisions until spindle disassembly in meiosis II (30 min in *fzr1*Δ, Fig 2F; supplementary Movie S4 online), and they initiated an assembly of ectopic spindles thereafter (40 min, Fig 2F). Nuclear fragmentation as seen in *cuf2*Δ followed this spindle formation (95–115 min, supplementary Fig S1A online). Precise movie recording suggested that this fragmentation occurred through an attempt to segregate chromosomes by a spindle (supplementary Movie S5 online), which was never observed in WT cells (supplementary Movie S6 online).

To validate the terminology of 'meiosis III-like' division, we characterised the phenomenon further. In this division, cells displayed monopolar, V-shaped and bipolar spindles, although

bipolar spindles were seen less frequently and their spindle poles appeared to be duplicated insufficiently, presumably because each nucleus was haploid equivalent and inadequate for bipolar chromosome segregation (Fig 2F; see also supplementary Figs S1B,C online). When a bipolar spindle was formed, kinetochores visualised with Mis6-2mRFP were aligned on it, to either of the spindle poles in most cases but sometimes to the middle region (Fig 2F Inset-a; supplementary Fig S1B online), reinforcing that attempts to segregate chromosomes could occur in the meiosis III-like division. Quantitative analyses of the frequency of emergence for each type of spindle are summarised in supplementary Table S1 online. These ectopic spindles were assembled much later than the disassembly of the meiosis II spindles, when the forespore membrane completed nuclear constrictions (supplementary Fig S2 online). Taken together, it appears unlikely that they merely represent a remnant of spindles produced in meiosis II.

## *fzr1*$^+$ is a critical target of Cuf2

Given the resemblance of the mutant phenotypes, how is Cuf2 related to Fzr1 in the repression of meiosis III-like division? As Cuf2 is a transcription factor upregulated during meiosis, it is possible that Cuf2 boosts the *fzr1*$^+$ expression during meiosis, although a previous microarray analysis reported that deletion of *cuf2* did not significantly alter the *fzr1*$^+$ transcript level [13]. To investigate this possibility, we performed quantitative RT–PCR analysis of messenger RNAs purified from WT and *cuf2*Δ cells undergoing synchronized meiosis induced by the temperature-sensitive *pat1-114* mutation. In both strains, binucleate and tetranucleate cells peaked with similar kinetics after the temperature shift, confirming that the *cuf2*Δ mutant has no apparent defects in meiotic progression until meiosis II (Fig 3A). After the completion of meiosis II, abnormal nuclear fragmentation began to be seen in *cuf2*Δ ($\geqslant$5 nuclei, Fig 3A). The kinetics of *cuf2*Δ meiosis was also comparable to that of *fzr1*Δ reported previously [7,10], although the frequency of generation for $\geqslant$5 nuclei was not mentioned in these reports.

In quantitative RT–PCR analysis, we found that the transcription of *fzr1*$^+$ mRNA in *cuf2*Δ was decreased to 54% of that in WT during the transition phase from meiosis I to meiosis II (3–4 h, Fig 3B). In contrast, the expression of *cdc13*$^+$ (cyclin B) or *mes1*$^+$, important for the progression of meiosis II, did not differ significantly between the two strains throughout meiosis (Fig 3B).

To examine the direct involvement of Cuf2 in transcription of the *fzr1*$^+$ gene, chromatin immunoprecipitation (ChIP) assay was performed. Cuf2 tagged with five copies of the FLAG epitope (Cuf2–5FLAG) was efficiently co-precipitated with the promoter region of *fzr1*$^+$, but not with that of *cdc13*$^+$ or *mes1*$^+$ (Fig 3C). The *cuf2* mutant isolated in the original *sms* screen contained the R19Q mutation (substitution of arginine 19 to glutamine) within the putative DNA-binding domain inferred from a homology to Cuf1 [13]. Notably, the Cuf2(RQ)–5FLAG mutant protein did not significantly precipitate the *fzr1* promoter fragment (Fig 3C), strongly suggesting that Cuf2 directly activates transcription of *fzr1*$^+$ mRNA during meiosis, although it is unlikely to be the sole transcription factor for *fzr1*$^+$. Whether the residual binding of WT Cuf2 to the promoter region of *cdc13*$^+$ or *mes1*$^+$ is meaningful or not remains inconclusive. Cuf2–GFP localised to the chromatin structure in the nucleus in anaphase II, whereas the mutant protein Cuf2(RQ)–GFP dispersed to the cytoplasm (supplementary Fig S3 online). This was consistent to the ChIP results, as previous studies indicated that nucleoplasmic proteins, which do not associate with nuclear structures such as the chromatin or spindle, do not remain in the nucleus in anaphase II [14,15]. While the binucleate phenotype of the *mes1* mutant was suppressed by the *cuf2* mutation (Fig 1B,C), this suppression was cancelled when Fzr1 was artificially overexpressed from a multicopy plasmid (Fig 3D). Overexpression of Fzr1 in WT generated mono- and binucleate cells, but more than 50% cells possessed four nuclei in this case. Thus, we concluded that Fzr1 is a crucial target of Cuf2 to end the M-phase cycles in meiosis.

## Cdc13/cyclin B persists after meiosis II in *cuf2*Δ

We finally examined whether the reduction of *fzr1*$^+$ mRNA in *cuf2*Δ indeed resulted in a lack of Fzr1 protein during meiosis, and if this lack in turn stabilized the B-type cyclin Cdc13. In WT cells, the amount of Cuf2–GFP protein expressed from the endogenous promoter exhibited a spike at meiosis II (3.5–4.25 h, Fig 4A; supplementary Fig S3 online), which was relayed to a spike of Fzr1 protein expression from meiosis II onwards (3.5–5.0 h). This is consistent with the notion that Cuf2 boosts transcription of *fzr1*$^+$ mRNA (Figs 3A–C). The expression of Fzr1 limited to this timing caused constrained expression of Cdc13, which diminished during meiosis II (3.75–4.25 h, Fig 4A). In *cuf2*Δ cells, Fzr1 was less abundant and Cdc13 persisted until the end of meiosis II (4.75 h, Fig 4B), as in *fzr1*Δ cells [7,10]. In line with biochemical results, live-cell imaging detected accumulation of Cdc13 to SPBs during the meiosis III-like phase in both *cuf2*Δ and *fzr1*Δ cells, whereas in WT cells Cdc13 disappeared after anaphase II (Fig 4C). Securin/Cut2, another well-established substrate of APC/C, exhibited similar behaviour to Cdc13 (Fig 4D,E): it disappeared in anaphase II (15–35 min, Fig 4E) and reaccumulated to the ectopic spindle long after meiosis II was terminated (70–85 min).

Taken together, these results suggest that the meiosis III-like division is an additional round of nuclear division, rather than just an aberrant extension of meiosis II. This was supported by the observations that microtubules, cyclin and securin similarly repeated synchronous disappearance and reappearance after meiosis II, and that they led to irregular SPB duplication and chromosome segregation in the next round.

## The mechanism of terminating the meiotic cycle

This study revealed the mechanism by which meiotic cells terminated the consecutive nuclear divisions after meiosis II, prohibiting the entry to meiosis III (Fig 4F). If Cdk1 activity was completely downregulated after anaphase I, as in mitotic exit, there would be a potential risk of early termination of meiosis without performing meiosis II. To avoid this, Mes1 inhibits APC/C to maintain Cdc13 until onset of meiosis II. Owing to this continual competency of Cdk1, cells in turn need to top up the APC/C activity after anaphase II to completely shut off the Cdk1 activity. Previous studies indicated that the meiosis-specific APC/C activator Fzr1/Mfr1 is required to degrade Cdc13 after meiosis II, and that this degradation is important for coordinated spore wall formation [7,10,11]. In *Saccharomyces cerevisiae* also, the Fzr1 homologue Ama1 has been shown to coordinate the exit from

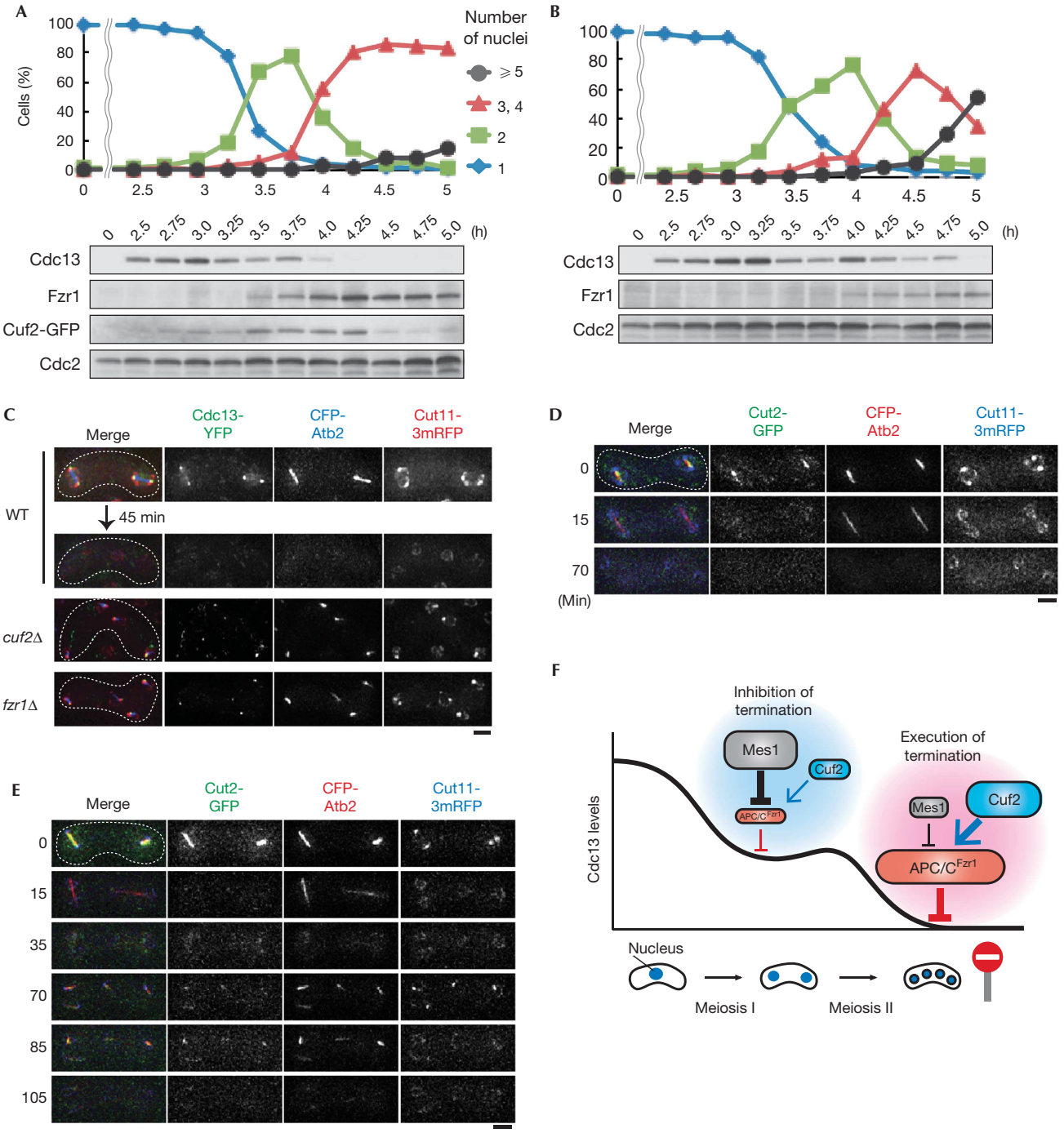


meiosis II with spore wall formation [16]. However, it remained unclear how significant Fzr1 is in termination of the meiotic cycle, and how Fzr1 expression is upregulated during meiosis. In this study, we demonstrated that Fzr1 is a critical factor responsible for the termination of meiosis, as evidenced by the meiosis III-like division frequently seen in *fzr1*Δ cells. Furthermore, we found that Fzr1 is upregulated at the transcriptional level by the transcription factor Cuf2. Thus, timely Cdc13 proteolysis promoted by the Cuf2–Fzr1–APC/C pathway prevents cells from entering a third division, besides facilitating coordinated spore wall formation, to ensure the exit from meiosis II.

Some ascomycete species, including *Schizosaccharomyces japonicus*, undergo post-meiotic mitosis to produce eight spores. The occurrence of meiosis III-like division in *S. pombe* revealed in this study suggests that the extra division in these species might also be assured by a mechanism to lower the APC/C activity. Meiosis III-type phenomena have been observed in mouse, bovine, plant and ascidian meioses [17–20]. In mouse and

◀ **Fig 4** | Cuf2 is required for timely proteolysis of Cdc13/Cyclin B at the termination of meiosis. (**A**,**B**) Cdc13 was more stable in *cuf2*Δ cells than in WT cells. Protein extracts were prepared at each time point from *cuf2*$^{+}$–GFP (**A**) and *cuf2*Δ (**B**) cultures undergoing synchronized meiosis. The number of nuclei per cell was counted at each time point ($n > 200$). Proteins indicated were detected by western blotting. (**C**) Images of a single WT cell undergoing meiosis II, and a *cuf2*Δ and a *fzr1*Δ cell undergoing meiosis III-like division. Green, Cdc13–YFP (cyclin B); blue, CFP–Atb2 (microtubules); and red, Cut11–3mRFP (nuclear envelope). Note that Cut11–3mRFP, which is known to localise to SPBs in addition to the nuclear envelope during M phases, was concentrated at the SPBs forming ectopic spindles after meiosis II. (**D**,**E**) Cut2/Securin reaccumulated and localised to the ectopic spindles that emerged after meiosis II in *fzr1*Δ. WT (**D**) and *fzr1*Δ (**E**) cells expressing Cut2-GFP (securin; green), CFP-Atb2 (microtubules; red) and Cut11-3mRFP (nuclear envelope; blue) were filmed from meiosis II. (**F**) A model illustrating how cells terminate meiosis through the regulation of APC/C. During the transition from meiosis I to meiosis II, APC/C–Fzr1 is inhibited by Mes1 to maintain Cdc13 levels (inhibition of termination). At late meiosis II, however, Fzr1 increased by the function of Cuf2 executes complete degradation of Cdc13, so that no more meiotic divisions might occur (execution of termination). APC/C, anaphase-promoting complex/cyclosome; CFP, cyan fluorescent protein; GFP, green fluorescent protein; mRFP, monomeric red fluorescent protein; SPB, spindle pole body; WT, wild type; YFP, yellow fluorescent protein. Scale bar, 2 μm.

ascidian meioses, proper regulation of Mos–MAPK activity is essential to avoid the entry to meiosis III [19,21,22], although this is unlikely to be a universal mechanism according to studies in other species, including amphibians [23]. In *Arabidopsis thaliana*, initiation of meiosis II is regulated by a close homologue of fission yeast Mes1 [24]. As yeasts and plants do not appear to have the Mos–MAPK pathway that regulates APC/C, the transcription machinery conducted by meiotic transcription factors including Cuf2 might have developed to enhance the APC/C activity to terminate meiosis in these organisms.

## METHODS

**Yeast strains and genetic methods.** Strains used in this study are listed in supplementary Table S2 online. Standard PCR-based gene targeting methods were used to create gene disruptants and epitope-tagged strains, in which the tagged gene replaced the endogenous gene [25–28]. Sporulation agar medium was used for the induction of mating, meiosis and sporulation of homothallic ($h^{90}$) strains. To identify the *sms1* and *sms5* genes of the mutant, we performed whole-genome sequencing using GAIIx (Illumina), the experimental conditions of which are described in supplementary Methods online.

**Microscopy.** Live-cell imaging was performed with the DeltaVision-SoftWoRx system (GE Healthcare) as described previously [28]. Cells undergoing mating and meiosis on sporulation agar were mounted onto glass-bottomed dishes (Matsunami) precoated with lectin, and the dishes were filled with liquid minimal medium without nitrogen. Images were acquired as serial sections along the z-axis and stacked using the 'quick projection' algorithm in SoftWoRx. For images in Fig 1B, fixed cells were stained with DAPI (Wako Pure Chemicals). DIC and DAPI images were taken with an AxioPlan 2 fluorescence microscope (Zeiss) operated by the SlideBook software (Leeds Precision).

**Induction of synchronized meiosis.** To induce synchronized meiosis, the diploid *pat1-114*+*mat-Pc* system was employed [29–31]. In brief, cells grown to the mid-log phase in the rich medium YE (yeast extract) were washed and transferred to minimal medium without nitrogen. After incubation at 25 °C for 7 h to arrest cells at G1 phase, temperature was shifted up to 34 °C to inactivate Pat1 kinase. Aliquots of cells were then collected at the time indicated and lysed for biochemical analyses. To score the number of nuclei in each cell, cells were fixed with methanol and stained with DAPI (4′,6-diamidino-2-phenylindole; Wako Pure Chemicals).

**Biochemistry and quantitative PCR techniques.** Details of biochemical experiments using RNA and protein extraction, ChIP assays, and quantitative PCR assays are described in supplementary Methods online. Oligos used for quantitative PCR assays are listed in supplementary Table S3 online.

**Supplementary information** is available at EMBO *reports* online (http://www.emboreports.org).

ACKNOWLEDGEMENTS

We are grateful to Hiro Yamano, Eishi Noguchi, Hiroshi Murakami, Taro Nakamura, Yoshiyuki Imai, Andreas Anders and Ken Sawin for materials and support. Y.A. is a research fellow (DC) of the Japan Society for the Promotion of Science (JSPS), and we thank Yuichi Iino for encouragement. This work was supported by the Grant-in-Aids for Scientific Research on Priority Areas 'Cell Proliferation Control' from MEXT (Ministry of Education, Culture, Sports, Science, and Technology; to M.S.) and for Specially Promoted Research and Scientific Research (S) from JSPS (Japan Society for the Promotion of Science; to M.Y.), and by the Global COE Programme (Integrative Life Science Based on the Study of Biosignaling Mechanisms), MEXT, Japan.

*Author contributions:* Experiments for the data presented were designed and performed by Y.A. supervised by M.S., A.Y. and M.Y. The initial stage of this study was supported by K.A., M.M. (*fzr1* observation) and Y.K. (*sms* mutant isolation). Y.A., M.S. and M.Y. wrote the manuscript.

CONFLICT OF INTEREST

The authors declare that they have no conflict of interest.

REFERENCES

1. Marston AL, Amon A (2004) Meiosis: cell-cycle controls shuffle and deal. *Nat Rev Mol Cell Biol* **5:** 983–997
2. Peters JM (2006) The anaphase promoting complex/cyclosome: a machine designed to destroy. *Nat Rev Mol Cell Biol* **7:** 644–656
3. Pesin JA, Orr-Weaver TL (2008) Regulation of APC/C activators in mitosis and meiosis. *Annu Rev Cell Dev Biol* **24:** 475–499
4. Verlhac MH, Terret ME, Pintard L (2010) Control of the oocyte-to-embryo transition by the ubiquitin-proteolytic system in mouse and *C. elegans*. *Curr Opin Cell Biol* **22:** 758–763
5. Izawa D, Goto M, Yamashita A, Yamano H, Yamamoto M (2005) Fission yeast Mes1p ensures the onset of meiosis II by blocking degradation of cyclin Cdc13p. *Nature* **434:** 529–533
6. Kimata Y, Trickey M, Izawa D, Gannon J, Yamamoto M, Yamano H (2008) A mutual inhibition between APC/C and its substrate Mes1 required for meiotic progression in fission yeast. *Dev Cell* **14:** 446–454
7. Blanco MA, Pelloquin L, Moreno S (2001) Fission yeast *mfr1* activates APC and coordinates meiotic nuclear division with sporulation. *J Cell Sci* **114:** 2135–2143

8. Cooper KF, Mallory MJ, Egeland DB, Jarnik M, Strich R (2000) Ama1p is a meiosis-specific regulator of the anaphase promoting complex/cyclosome in yeast. *Proc Natl Acad Sci USA* **97:** 14548–14553
9. Yamamoto A, Kitamura K, Hihara D, Hirose Y, Katsuyama S, Hiraoka Y (2008) Spindle checkpoint activation at meiosis I advances anaphase II onset via meiosis-specific APC/C regulation. *J Cell Biol* **182:** 277–288
10. Kimata Y, Kitamura K, Fenner N, Yamano H (2011) Mes1 controls the meiosis I to meiosis II transition by distinctly regulating the anaphase-promoting complex/cyclosome coactivators Fzr1/Mfr1 and Slp1 in fission yeast. *Mol Biol Cell* **22:** 1486–1494
11. Asakawa H, Kitamura K, Shimoda C (2001) A novel Cdc20-related WD-repeat protein, Fzr1, is required for spore formation in *Schizosaccharomyces pombe*. *Mol Genet Genomics* **265:** 424–435
12. Mata J, Lyne R, Burns G, Bähler J (2002) The transcriptional program of meiosis and sporulation in fission yeast. *Nat Genet* **32:** 143–147
13. Ioannoni R, Beaudoin J, Lopez-Maury L, Codlin S, Bähler J, Labbé S (2012) Cuf2 is a novel meiosis-specific regulatory factor of meiosis maturation. *PLoS ONE* **7:** e36338
14. Arai K, Sato M, Tanaka K, Yamamoto M (2010) Nuclear compartmentalization is abolished during fission yeast meiosis. *Curr Biol* **20:** 1913–1918
15. Asakawa H, Kojidani T, Mori C, Osakada H, Sato M, Ding DQ, Hiraoka Y, Haraguchi T (2010) Virtual breakdown of the nuclear envelope in fission yeast meiosis. *Curr Biol* **20:** 1919–1925
16. Diamond AE, Park JS, Inoue I, Tachikawa H, Neiman AM (2009) The anaphase promoting complex targeting subunit Ama1 links meiotic exit to cytokinesis during sporulation in Saccharomyces cerevisiae. *Mol Biol Cell* **20:** 134–145
17. Kubiak JZ (1989) Mouse oocytes gradually develop the capacity for activation during the metaphase II arrest. *Dev Biol* **136:** 537–545
18. Ross KJ, Fransz P, Armstrong SJ, Vizir I, Mulligan B, Franklin FC, Jones GH (1997) Cytological characterization of four meiotic mutants of *Arabidopsis* isolated from T-DNA-transformed lines. *Chromosome Res* **5:** 551–559
19. Dumollard R, Levasseur M, Hebras C, Huitorel P, Carroll M, Chambon JP, McDougall A (2011) Mos limits the number of meiotic divisions in urochordate eggs. *Development* **138:** 885–895
20. Li GP, Liu Y, Bunch TD, White KL, Aston KI (2005) Asymmetric division of spindle microtubules and microfilaments during bovine meiosis from metaphase I to metaphase III. *Mol Reprod Dev* **71:** 220–226
21. Araki K, Naito K, Haraguchi S, Suzuki R, Yokoyama M, Inoue M, Aizawa S, Toyoda Y, Sato E (1996) Meiotic abnormalities of c-*mos* knockout mouse oocytes: activation after first meiosis or entrance into third meiotic metaphase. *Biol Reprod* **55:** 1315–1324
22. Verlhac MH, Kubiak JZ, Weber M, Geraud G, Colledge WH, Evans MJ, Maro B (1996) Mos is required for MAP kinase activation and is involved in microtubule organization during meiotic maturation in the mouse. *Development* **122:** 815–822
23. Ješeta M, Bodart J-FL (2012) Comparing pig and amphibian oocytes: methodologies for aneuploidy detection and complementary lessons for mapk involvement in meiotic spindle morphogenesis. In *Aneuploidy in Health and Disease*, Storchova Z, (ed.) pp 193–216. Rijeka, Croatia: InTech
24. Cromer L *et al* (2012) OSD1 promotes meiotic progression via APC/C inhibition and forms a regulatory network with TDM and CYCA1;2/TAM. *PLoS Genet* **8:** e1002865
25. Noguchi C, Garabedian MV, Malik M, Noguchi E (2008) A vector system for genomic FLAG epitope-tagging in *Schizosaccharomyces pombe*. *Biotechnol J* **3:** 1280–1285
26. Bähler J, Wu JQ, Longtine MS, Shah NG, McKenzie A 3rd, Steever AB, Wach A, Philippsen P, Pringle JR (1998) Heterologous modules for efficient and versatile PCR-based gene targeting in *Schizosaccharomyces pombe*. *Yeast* **14:** 943–951
27. Sato M, Dhut S, Toda T (2005) New drug-resistant cassettes for gene disruption and epitope tagging in *Schizosaccharomyces pombe*. *Yeast* **22:** 583–591
28. Sato M, Toya M, Toda T (2009) Visualization of fluorescence-tagged proteins in fission yeast: the analysis of mitotic spindle dynamics using GFP-tubulin under the native promoter. *Methods Mol Biol* **545:** 185–203
29. Kakui Y, Sato M, Tanaka K, Yamamoto M (2011) A novel fission yeast *mei4* mutant that allows efficient synchronization of telomere dispersal and the first meiotic division. *Yeast* **28:** 467–479
30. Funaya C *et al* (2012) Transient structure associated with the spindle pole body directs meiotic microtubule reorganization in *S. pombe*. *Curr Biol* **22:** 562–574
31. Yamamoto A, Hiraoka Y (2003) Monopolar spindle attachment of sister chromatids is ensured by two distinct mechanisms at the first meiotic division in fission yeast. *EMBO J* **22:** 2284–2296